

УДК 539.12...173

NEW METHOD OF FAST SIMULATION FOR A HADRON CALORIMETER RESPONSE¹

Y. Kulchitsky^a, *J. Šutiak*^b, *S. Tokár*^b, *T. Ženiš*^b

^a On leave from B. I. Stepanov Institute of Physics,
National Academy of Sciences, Minsk

^b Comenius University, Bratislava

In this work we present the new method of a fast Monte-Carlo simulation of a hadron calorimeter response. It is based on the three-dimensional parameterization of the hadronic shower obtained from the ATLAS TILECAL test beam data and GEANT simulations. A new approach of including the longitudinal fluctuations of hadronic shower is described. The obtained results of the fast simulation are in good agreement with the TILECAL experimental data.

Разработан новый метод быстрого моделирования отклика адронного калориметра. Метод базируется на трехмерной параметризации адронного ливня, полученной в результате анализа экспериментальных данных с адронного тайл-калориметра эксперимента АТЛАС, и результатах моделирования с использованием программы GEANT. Предложен новый механизм для моделирования продольных флуктуаций энергии в адронном ливне. Результаты быстрого моделирования хорошо согласуются с экспериментальными данными, полученными для TILECAL.

*In memory of our friend
Dr. Victor Rumyantsev.*

INTRODUCTION

Hadron calorimetry is an important part of the high-energy physics experiments. Simulation of calorimeter response is an integral part of a calorimeter design and development. It is also inevitable to simulate calorimeter response as a part of full detector response for treating different physics processes to be studied by an experimental setup.

The well-known way of the simulation of hadron calorimeter response is to use the GEANT detector simulation package [1]. The GEANT simulations are quite time-consuming, and in many cases it is more convenient to use the fast simulation methods. In this work we present the fast simulation method, which does not take into account the concrete physical interactions, except for a few the most energetic collisions at the beginning of the shower development. The fast Monte Carlo (MC) is based on a three-dimensional parameterization of hadron shower development obtained from the ATLAS TILECAL test beam data [2–4] and GEANT simulations.

¹ Presented at the International ATLAS Collaboration Conference, October 2002, CERN, Geneva, Switzerland.

1. THE TILE CALORIMETER

The presented work is tightly connected to the hadronic Tile Calorimeter prototype [2, 5, 6] of the ATLAS collaboration. However, the method can be applied to any other sampling calorimeter.

The Tile Calorimeter [5, 7, 8] is a sampling device made out of steel and scintillating tiles, as absorber and active material, respectively (Fig. 1). The absorber structure is a laminate of steel plates of various dimensions stacked along Z . The basic geometrical element of the stack is what we call a period. It consists of a set of two master plates (large trapezoidal steel plates, 5 mm thick, spanning along the entire X dimension) and one set of spacer plates (small trapezoidal steel plates, 4 mm thick, 10 cm wide along X).

Each stack, called module, spans $2\pi/64$ in the azimuthal angle (Y dimension), 100 cm in the Z direction and 180 cm in the X direction (about nine interaction lengths, λ_I , or about 80 effective radiation lengths, X_0). Each module has 57 repeated periods. The module front face, exposed to the beam particles, covers 100×20 cm. The scintillating tiles are made out of polystyrene material 3 mm in thickness, doped with scintillator. The iron to scintillator ratio is 4.67 : 1 by volume. The calorimeter thickness along the beam direction at the incidence angle of $\Theta = 10^\circ$ (the angle between the incident particle direction and the normal to the calorimeter front face) corresponds to 1.49 m of iron equivalent length. The prototype Tile Calorimeter used for this study is composed of five modules stacked in the Y direction, as shown in Fig. 2.

The modules are divided into five segments along Z and they are also longitudinally segmented (along X) into four depth segments.

The readout cells have a lateral dimension of 200 mm along Z , and longitudinal dimensions of 300, 400, 500, 600 mm for depth segments 1–4, corresponding to 1.5, 2, 2.5 and 3 λ_I at $\Theta = 0^\circ$, respectively. Along Y , the cell sizes vary between about 200 and 370 mm depending on the X coordinate.

The calorimeter was placed on a scanning table that allowed movement in any direction. Upstream of the calorimeter, a trigger counter telescope (S1, S2, S3) was installed, defining a beam spot approximately 20 mm in diameter. Two delay-line wire chambers (BC1 and BC2), each with (Z, Y) readout, allowed the impact point of beam particles on the calorimeter face to be reconstructed to better than ± 1 mm. Additional scintillators for the muon detection were placed behind and on the side of the calorimeter prototype to measure the longitudinal and lateral hadronic shower leakage. The «Back muon wall» (800×800 mm) is shown

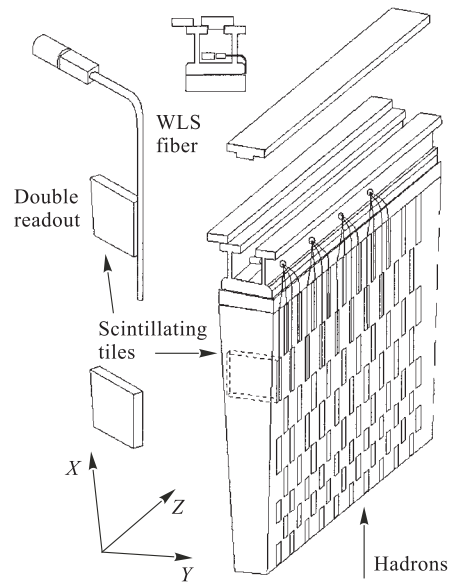


Fig. 1. Conceptual design of a Tile Calorimeter module

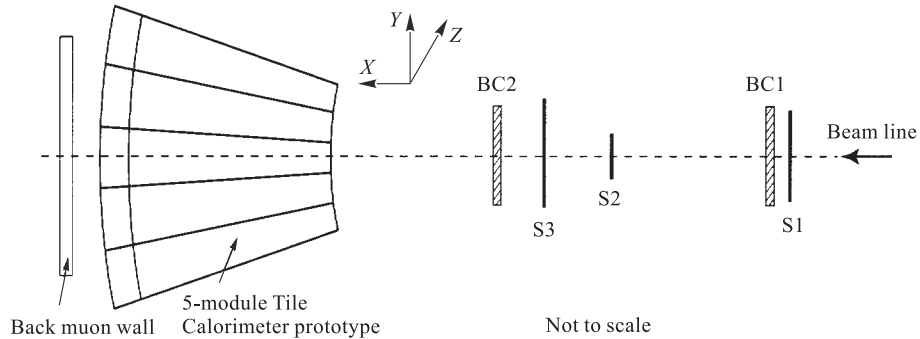


Fig. 2. Schematic layout of the experimental setup (side view): S1, S2 and S3 are beam trigger scintillators; BC1 and BC2 are (Z, Y) proportional chambers

in Fig. 2. The other scintillators were placed on the positive Z side (400×1150 mm) and are not seen in Fig. 2.

2. THE PRINCIPLE OF THE FAST SIMULATIONS

The method of fast MC presented here follows the ideas published in the work of Grindhammer et al. [9] and is suggested for sampling calorimeters. In our approach, a different method of including the longitudinal profile fluctuations has been employed.

The shower that develops beginning at a certain depth of the detector is represented by a set of *energy spots*. These spots are distributed according to a known spatial distribution function. The number of spots deposited in the active medium N_A is a random variable with Poisson distribution function, so its relative standard deviation is $1/\sqrt{N_A}$. As the amount of detected energy is proportional to the number of spots in the active medium, the relative fluctuations of detected energy are also $1/\sqrt{N_A}$. We will show later how to determine the appropriate number of spots for a given energy resolution.

2.1. Components of Hadronic Shower. Due to production of π^0 mesons which decay always into electromagnetic particles, the shower consists of two subshowers — electromagnetic (EM) subshower and pure hadronic (HD) one. Accordingly, the energy distribution function has two parts. The shape of the distribution function varies from event to event, so it is fixed for each event separately. In noncompensated sampling calorimeters, the ratio between signal response for the electromagnetic and pure hadronic part of shower is given by the well-known e/h ratio, e. g., [10, 11]. To obtain a signal value comparable with the experiment, energy of the spots representing electromagnetic (hadronic) subshower is calibrated by the value e (h). The algorithm of the fast simulation program may be written as follows:

1. To fix the spatial energy distribution function.
2. To find the origin of shower (vertex) and to deposit the ionization energy losses of incident particle up to the interaction vertex.
3. To decide whether the current spot will be distributed according to the electromagnetic or hadronic part of distribution function.

4. To find the position of the energy spot and decide whether it is absorbed in the active or passive medium.

5. If absorbed by the active medium, the value of signal (either electromagnetic or hadronic) is appropriately modified.

The steps 2–5 are repeated for all the spots of the current shower. Calculation of the spatial energy distribution function is done for each event individually.

2.2. The Size of Energy Spots. In the previous chapter we mentioned that the number of energy spots is related to the calorimeter energy resolution. The usual parameterization of the resolution is

$$\frac{\sigma_E}{E} = \frac{a}{\sqrt{E}} \oplus b, \quad (1)$$

where a is the stochastic coefficient representing the combined effect of sampling and photostatistic fluctuations. The coefficient b (constant term) characterizes nonuniformities of a calorimeter. For this calorimeter their values are $a = 0.55$ and $b = 0.03$. In the sampling calorimeters, only a part of energy is deposited in the active medium and detected. The sampling fraction s_f for the sampling calorimeters is defined as a ratio of the energy deposited by minimum ionizing particle (mip) in the active medium E_A and the total energy deposited E [12, p. 109]:

$$s_f = \frac{E_A}{E}. \quad (2)$$

In this explanation, we assume that the shower consists of mips — this assumption is not principal for the energy resolution.

Our scenario for treating the shower is as follows: the energy of an incident particle is divided into N energy spots each with the energy q_{eff} and distributed over the volume of the calorimeter. The probability that a spot is absorbed in the active medium is s_f . On average, N_A of them are absorbed in the active medium:

$$N_A = s_f N. \quad (3)$$

N_A is a random variable obeying Poisson law; therefore, its standard deviation is $\sqrt{N_A}$. If we do not take into account the constant term, then the energy resolution is determined by the relative standard deviation of N_A , because E_A is proportional to N_A :

$$\frac{\sigma_E}{E} = \frac{\sqrt{N_A}}{N_A}. \quad (4)$$

From (1)–(4) one can find the appropriate number of energy spots:

$$N = \frac{E}{a^2 s_f}, \quad (5)$$

and the size of the energy spot:

$$q_{\text{eff}} = a^2 s_f. \quad (6)$$

The constant term can be included by multiplying the amount of energy deposited in each cell in one event by the factor $(1 + b')$, where b' is normally distributed random number with $\sigma = b$ and $\mu = 0$.

3. THE SHOWER PROFILE

We have studied the profile of a hadronic shower using the full GEANT simulations [1] as well as the data obtained at the test beam experiments with the prototype of the hadronic calorimeter of the ATLAS collaboration [2,5]. We carried out simulations of response on π^- with incident energies of 20, 50, 100, 200, 300 and 500 GeV. The experimental setup was the same as in the test beam measurements. The test beam data were then used for tuning up and testing the fast MC.

In this work, the following coordinate system has been chosen. The origin of the coordinate system is put to the shower origin (the first hadronic interaction), and the x axis is parallel to the beam line. We assume that the shower is symmetrical around this axis, and thus the average energy density function is only a function of the distance from the shower axis $r = \sqrt{y^2 + z^2}$ and the longitudinal coordinate x :

$$\Psi(x, r) = \frac{1}{E_0} \frac{dE(x)}{dx} \phi(x, r), \quad (7)$$

where $\Psi(x, r)$ is a joint probability density function (p. d. f.); $dE(x)/dx$ is a marginal p. d. f. and $\phi(x, r)$ is a conditional p. d. f. E_0 is the total energy deposited. Since the shapes of the electromagnetic and hadronic subshowers differ substantially, we need to study them separately. The joint p. d. f. function $\Psi(x, r)$ is thus a superposition of functions $\Psi_e(x, r)$ and $\Psi_h(x, r)$ corresponding to the electromagnetic and hadronic component, respectively [13]:

$$\Psi(x, r) = w\Psi_e(x, r) + (1 - w)\Psi_h(x, r). \quad (8)$$

The parameter w represents the contribution of the electromagnetic subshower to the full calorimeter signal. It is determined by the total energy fraction of the π^0 mesons produced. The relation between the mean values $\langle w \rangle$ and $\langle f_{\pi^0} \rangle$ is the following:

$$\langle w \rangle = \frac{e/h \langle f_{\pi^0} \rangle}{(e/h - 1) \langle f_{\pi^0} \rangle + 1}. \quad (9)$$

The method of calculation of the e/h value is described in [10,11]. The dependence of $\langle f_{\pi^0} \rangle$ on the total energy E can be parameterized by the following formula [14]:

$$\langle f_{\pi^0} \rangle = 0.11 \ln(E), \quad (10)$$

where E is the energy of an incident hadron in gigaelectronvolts. For a given total energy, the parameter w fluctuates significantly. We have found the shape of its p. d. f. using the GEANT simulation. It can be approximated by the function (Fig. 3):

$$p(w) = \frac{(w - w_0)^{\alpha_w - 1} e^{-(w - w_0)/\beta_w}}{\beta_w^{\alpha_w} \Gamma(\alpha_w)}. \quad (11)$$

The parameters α_w and β_w were found by fitting the simulated electromagnetic energy distribution. The mean value of this p. d. f. is $\langle w \rangle = w_0 + \alpha_w \beta_w$. Since the GEANT simulations do not reproduce the correct e/h ratio [15], we calculated the parameter w_0 from the equations (9) and (10) using the value $e/h = 1.36$ from experiment [10]. The fast MC then reproduces correctly the ratio between electromagnetic and hadronic energy.

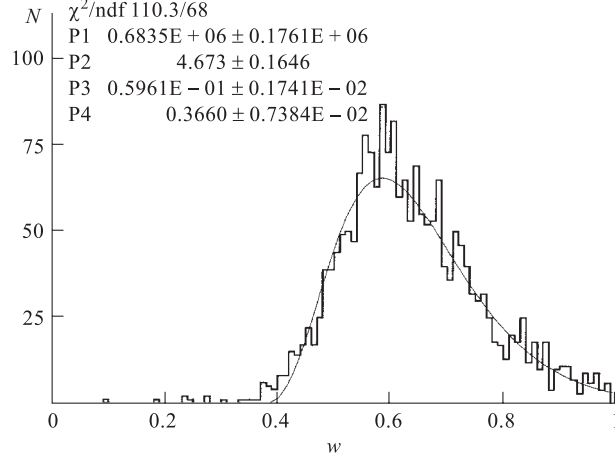


Fig. 3. Distribution of the events as a function of the parameter w (9) — the ratio of the pure electromagnetic signal to the total one at 100 GeV

3.1. The Shower Origin. The probability that a hadron crosses a distance h in a given medium without interaction is given by

$$p(h) = \frac{e^{-h/\lambda_I}}{\lambda_I}, \quad (12)$$

where λ_I is the interaction length. This function is used to find the distance between the front face of the calorimeter and the primary shower vertex.

3.2. The Mean Longitudinal Profile. There is a well-known parameterization of longitudinal shower profile suggested by Bock et al. [13]:

$$\frac{dE(x)}{dx} = E_0 \left\{ w G \left(\frac{x}{X_0}, \alpha_e, \beta_e \right) + (1-w) G \left(\frac{x}{\lambda_I}, \alpha_h, \beta_h \right) \right\}, \quad (13)$$

where $G(x, \alpha, \beta)$ is the gamma distribution function:

$$G(x, \alpha, \beta) = \frac{x^{\alpha-1} e^{-x/\beta}}{\beta^\alpha \Gamma(\alpha)}. \quad (14)$$

The first term in (13) corresponds to the electromagnetic component and the second term to the hadronic component; X_0 and λ_I are the radiation and interaction lengths, $\alpha_e, \beta_e, \alpha_h, \beta_h$ are the profile parameters.

In the present work, we used modified function for describing the electromagnetic profile. The shape of the electromagnetic profile is determined by the places of birth of π^0 mesons and by their energies. According to the full MC simulations, the (mean) shape of the function $dE_{\pi^0}/dx(x)$, describing the total π^0 energy produced in strong interactions on a unit distance, is as follows (Fig. 4):

$$\frac{dE_{\pi^0}}{dx}(x) = \begin{cases} E_1 \delta(x) & x = 0 \\ E_2 \frac{\exp(-x/\lambda_{\pi^0})}{\lambda_{\pi^0}} & x > 0 \end{cases}, \quad (15)$$

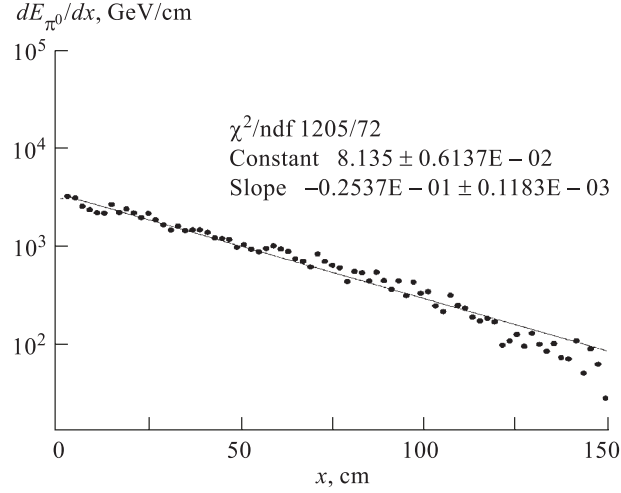


Fig. 4. The distribution of the energy density function $dE_{\pi^0}(x)/dx$ for π^0 (15) as a function of the longitudinal x coordinate at 100 GeV

i. e., a large fraction of the π^0 energy is produced in the first interaction and then the amount of energy per unit distance decreases exponentially. This exponential decrease scales with interaction length, while the shower produced by π^0 from the first interaction scales with radiation length. This is the reason why the use of the first term in (13) is not appropriate for describing the electromagnetic component. On the other hand, this term should be adequate for the description of local electromagnetic shower initiated by π^0 produced at a given depth. The parameters α_e and β_e are energy-dependent and also vary from case to case for a given energy. However, the energy dependence is weak ($\alpha_e, \beta_e \sim f(\ln E)$). We assume them to be constant for a given incident energy. The longitudinal profile of electromagnetic component is then a convolution of the functions (14) and (15):

$$\frac{dE_e}{dx}(x) = \int_0^x \frac{dE_{\pi^0}}{dx}(t) G(x-t, \alpha_e, \beta_e) dt. \quad (16)$$

Fitting the simulated electromagnetic component profile by this function, we found appropriate α_e and β_e for each incident energy (Fig. 5, a). The values for different energies are given in Table 1.

Table 1. The longitudinal hadronic shower profile parameters

$E_{\text{inc}}, \text{ GeV}$	20	50	100	200	500
α_e	2.83 ± 0.03	3.14 ± 0.04	3.39 ± 0.03	3.54 ± 0.04	3.93 ± 0.04
$\beta_e, \text{ cm}$	4.91 ± 0.11	5.00 ± 0.09	5.04 ± 0.15	5.18 ± 0.09	5.28 ± 0.12
$\lambda_{\pi^0}, \text{ cm}$	30.01 ± 0.15	34.6 ± 0.21	38.61 ± 0.19	42.65 ± 0.31	45.91 ± 0.35
α_h	1.33 ± 0.11	1.52 ± 0.08	1.65 ± 0.13	1.77 ± 0.18	1.91 ± 0.10
$\beta_h, \text{ cm}$	34.2 ± 3.1	36.4 ± 4.2	37.55 ± 3.6	38.67 ± 4.1	40.25 ± 3.5

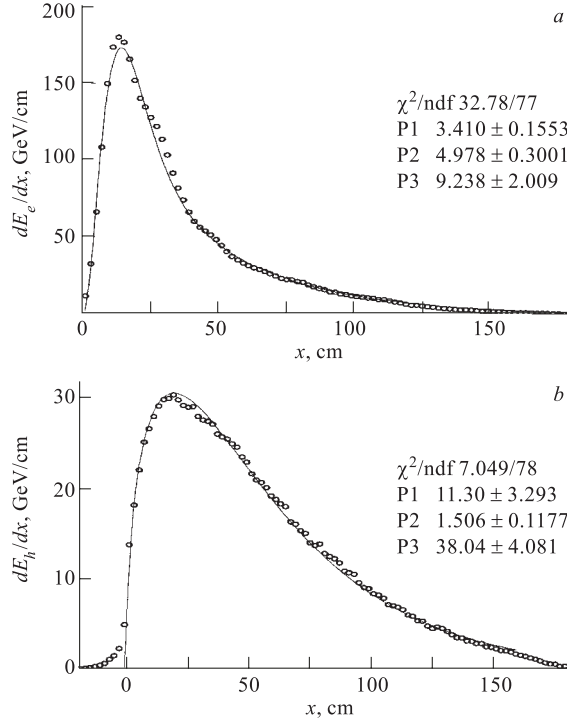


Fig. 5. Distribution of the longitudinal profile of electromagnetic component $dE_e(x)/dx$ (16) (a) and of hadronic component $dE_h(x)/dx$ (19) (b) of hadronic showers at 100 GeV as a function of the longitudinal coordinate

The average profile of the hadronic component $dE_h/dx(x)$ is well described by the second term in (13). The values of parameters α_h and β_h were found by fitting the simulated hadronic profile (Fig. 5, b). Their values are given in Table 1.

3.3. Fluctuations of the Longitudinal Profile. *3.3.1. Hadronic Component.* In our approach, we rely on the assumption that the shape of each particular shower, in case of the hadronic component, is determined by several most energetic particles that are produced in the first spallation interaction. These particles are mostly pions, protons and neutrons. They move approximately in parallel to the beam axes and carry the major part of the incident energy [12, p. 68–77]. They interact in different spatial points giving rise with partial subshowers. The fact that a hadronic shower consists of several partial subshowers starting at different points is the main source of the event-by-event fluctuations.

The probability that a primary vertex particle crosses the distance x before it undergoes an interaction with a nucleus is given by (we do not consider the π^0 mesons now)

$$p(x) = \frac{e^{-x/\lambda_i}}{\lambda_i}, \quad (17)$$

where λ_i is the corresponding interaction length for protons, neutrons, pions, etc. Each of these particles may start a subshower with a profile which can be described by the function:

$$\frac{dE_{\text{sub}}(x)}{dx} = G(x - x', \alpha'_h, \beta'_h), \quad (18)$$

where x' is the position of the subshower origin and α'_h, β'_h are parameters. The overall hadronic component profile for one particular event is thus a superposition of several subshowers, each starting at different depth from the primary hadronic shower vertex.

The average profile (accumulated through many events) should be a convolution of the functions (17) and (18). If we take $\lambda_i = \beta_h$ instead of considering the real interaction length value for each kind of particle, $\alpha'_h = \alpha_h - 1$ and $\beta'_h = \beta_h$, the result of the convolution is

$$\frac{dE_h}{dx}(x) = \int_0^x G(x - x', \alpha_h - 1, \beta_h) \frac{e^{-x'/\beta_h}}{\beta_h} dt = G(x, \alpha_h, \beta_h). \quad (19)$$

It means that we are able to reproduce correctly the average longitudinal hadronic component profile by superposing several partial subshowers in individual events.

We studied also the amount of energy carried by the fastest particles created in the first interaction and thus the energy of the subshowers initiated by them. In case of stable particles and neutrons their kinetic energy was considered, while in case of mesons the total energy was treated. The simulated spectrum of energies of primary vertex particles relative to the incident energy $f_i = E_i/E_{\text{inc}}$ is shown in Fig. 6. For parameterization of this spectrum we use the following function:

$$p(f_i) = N f_i^{c_h - 1} \exp(-f_i/d_h), \quad f_i \in [0, 1], \quad (20)$$

with the parameters c_h and d_h (see Table 2).

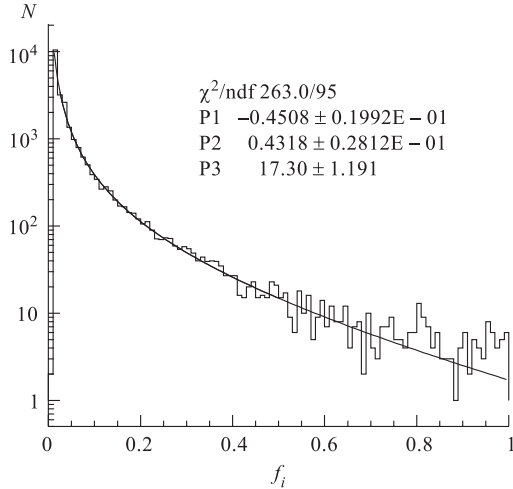


Fig. 6. The energy fraction spectrum of particles created in the first interaction in a 100-GeV shower (except for π^0)

In the fast MC program, the shape of the function $dE_h(x)/dx$ describing the longitudinal profile of the hadronic component for a single event is constructed as follows:

$$\frac{dE_h(x)}{dx} = \sum_i f_i G(x - x_i, \alpha_h - 1, \beta_h), \quad (21)$$

Table 2. The energy spectrum parameters for π^0 's and fast hadrons

E_{inc} , GeV	20	50	100	200	500
c_h	-0.082 ± 0.01	-0.23 ± 0.01	-0.42 ± 0.01	-0.52 ± 0.01	-0.64 ± 0.01
d_h	0.2	0.2	0.2	0.2	0.2
σ_{f_1}	0.63 ± 0.02	0.41 ± 0.02	0.38 ± 0.02	0.34 ± 0.02	0.32 ± 0.01
μ_{f_1}	0.58 ± 0.02	0.42 ± 0.02	0.36 ± 0.02	0.36 ± 0.02	0.31 ± 0.01
c_e	-0.26 ± 0.01	-0.40 ± 0.02	-0.40 ± 0.02	-0.48 ± 0.01	-0.59 ± 0.02
d_e	0.25 ± 0.02	0.24 ± 0.01	0.18 ± 0.01	0.16 ± 0.01	0.16 ± 0.01

where f_i is the energy fraction carried by i th primary vertex particle and x_i is its interaction point; G is the gamma distribution function.

The number of interactions is given by the condition

$$\sum_i f_i = 1. \quad (22)$$

3.3.2. Electromagnetic Component. The fluctuations of electromagnetic component can be included in a similar way. The situation is slightly different because the π^0 's decay immediately after being created. We have to consider π^0 's produced in the first interaction giving rise to a partial subshower starting at the vertex, as well as those produced in the higher generation interactions which produce subshowers that are distributed along the x axis.

According to GEANT simulation, the fraction f_1 of π^0 energy produced in the first interaction ($x = 0$) has the following p. d. f. (Fig. 7):

$$p(f_1) = N \exp\left(-\frac{(f_1 - \mu_{f_1})^2}{\sigma_{f_1}^2}\right), \quad f_1 \in [0, 1], \quad (23)$$

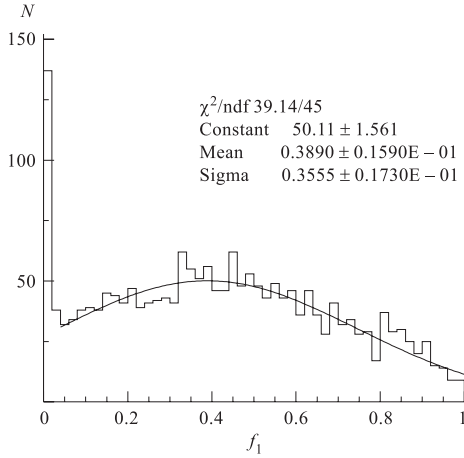


Fig. 7. The distribution of the fractional energy of π^0 produced in the first interaction in a 100-GeV shower

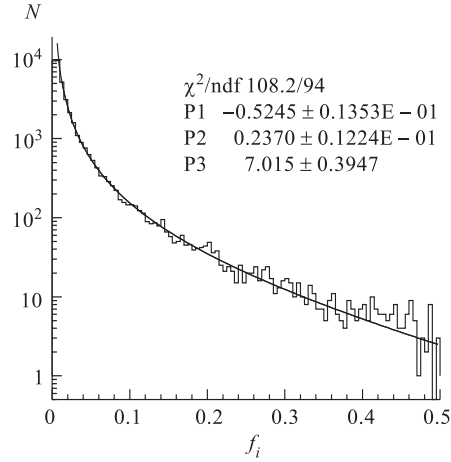


Fig. 8. The distribution of the fractional energy of π^0 's produced in one hadronic interaction different from the first one in a 100-GeV shower

where μ_{f1} and σ_{f1} are parameters (see Table 2). The p. d. f. of the fraction of π^0 energy f_i produced in one of the subsequent interactions is described by function (20) but with different parameters c_e and d_e (Fig. 8).

Similarly as in the case of the hadronic component, in the fast MC we can construct the electromagnetic profile by superposing the partial subshowers caused by π^0 created in individual interactions, each described by the function:

$$\frac{dE_{\text{sub}}(x)}{dx} = G(x - x', \alpha_e, \beta_e), \quad (24)$$

where x' is the position of the subshower origin and α_e, β_e are parameters, the same as in (16). The first subshower starts at the primary vertex, the starting points of subshowers from the higher generation of π^0 's match the positions of interactions of hadronic subshower particles:

$$\frac{dE_e(x)}{dx} = f_1 G(x, \alpha_e, \beta_e) + \sum_{i \geq 2} f_i G(x - x_i, \alpha_e, \beta_e), \quad (25)$$

where f_i is the fractional energy and x_i is the position of i th interaction producing π^0 's; G is the gamma distribution function. The number of interactions is given again by the condition (22).

3.4. The Radial Shower Profile. We studied the radial shower profile of both the electromagnetic and hadronic shower components using the GEANT simulations. The energy $\delta E_r(x, r)$ deposited in the «ring» with the centre on the x axis, the internal radius r and the volume $\Delta V = 2\pi r \Delta r \Delta x$ is

$$\delta E_r(x, r) = 2\pi \int_r^{r+\Delta r} \int_{x-\Delta x/2}^{x+\Delta x/2} E_0 \Psi(x, r) r dr dx \approx E_0 \Psi(x, r) 2\pi r \Delta r \Delta x. \quad (26)$$

The function $\delta E_r(x, r)/\delta r \delta x$ is related to the marginal p. d. f. $\phi(x, r)$ by the expression

$$\phi(x, r) = \frac{\delta E_r(x, r)}{2\pi r \Delta r \Delta x \frac{dE_h(x)}{dx}}. \quad (27)$$

The function $\Delta E_r(x, r)/\Delta r \Delta x$ was obtained for various depths x from 10 to 160 cm with step 10 cm separately for the electromagnetic and hadronic component. For each depth, it was parameterized by function:

$$\frac{\Delta E_r(x, r)}{\Delta r \Delta x} = c r^{\alpha_r(x)-1} e^{-r/\beta_r(x)}. \quad (28)$$

The examples of fits are shown in Fig. 9. In case of the electromagnetic component, we found the following approximations of the coefficients α_{re} and β_{re} as functions of shower depth (x coordinate) (Fig. 10, *a, b*):

$$\alpha_{re} = \alpha_{e0}(1 - 2e^{-x/\alpha_{e1}}), \quad (29)$$

$$\beta_{re} = \begin{cases} \beta_{e1} + \beta_{e2}x, & x \in [0, 30] \text{ cm}, \\ \beta_{e3} + \beta_{e4}x, & x \in [30, 180] \text{ cm}. \end{cases} \quad (30)$$

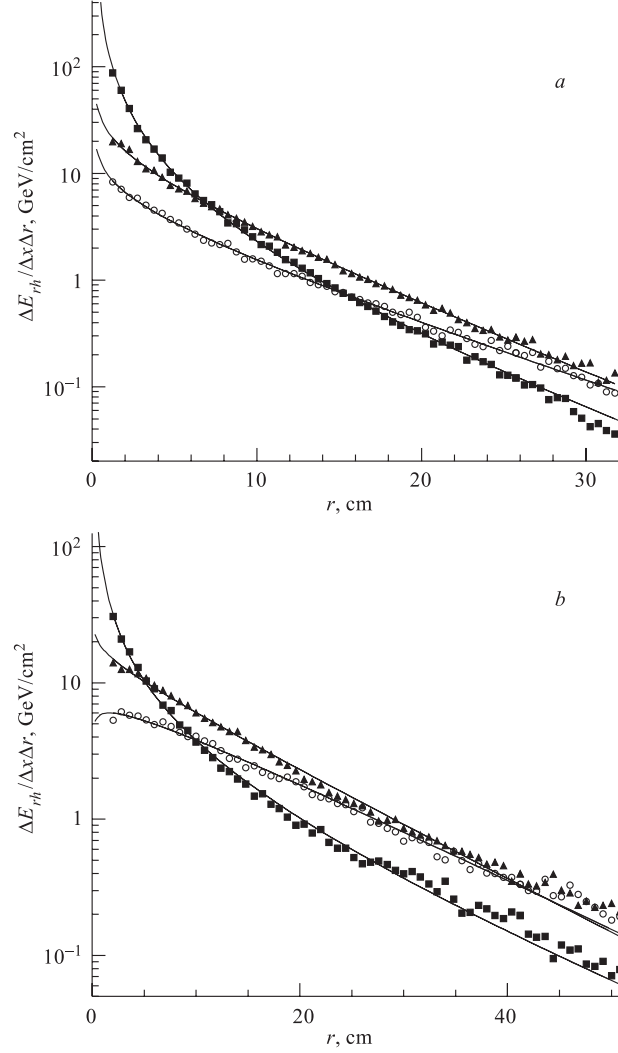


Fig. 9. The average simulated electromagnetic (a) and hadronic (b) radial shower profile in the three depths of the 100-GeV hadronic shower. ■ — $x = 10$ cm; ▲ — $x = 50$ cm; ○ — $x = 80$ cm

In the case of the hadronic component, the coefficients of x dependencies are as follows (Fig. 10, c, d):

$$\alpha_{rh} = \alpha_{h0} + \alpha_{h1} \ln x, \quad (31)$$

$$\beta_{rh} = \begin{cases} \beta_{h1} + \beta_{h2}x, & x \in [0, 30] \text{ cm}, \\ \beta_{h3} + \beta_{h4}x, & x \in [30, 180] \text{ cm}. \end{cases} \quad (32)$$

No fluctuations of $\phi(x, r)$ are included. The lateral shower fluctuations are therefore determined only by the fluctuations of w and by the random process of the energy spots distribution.

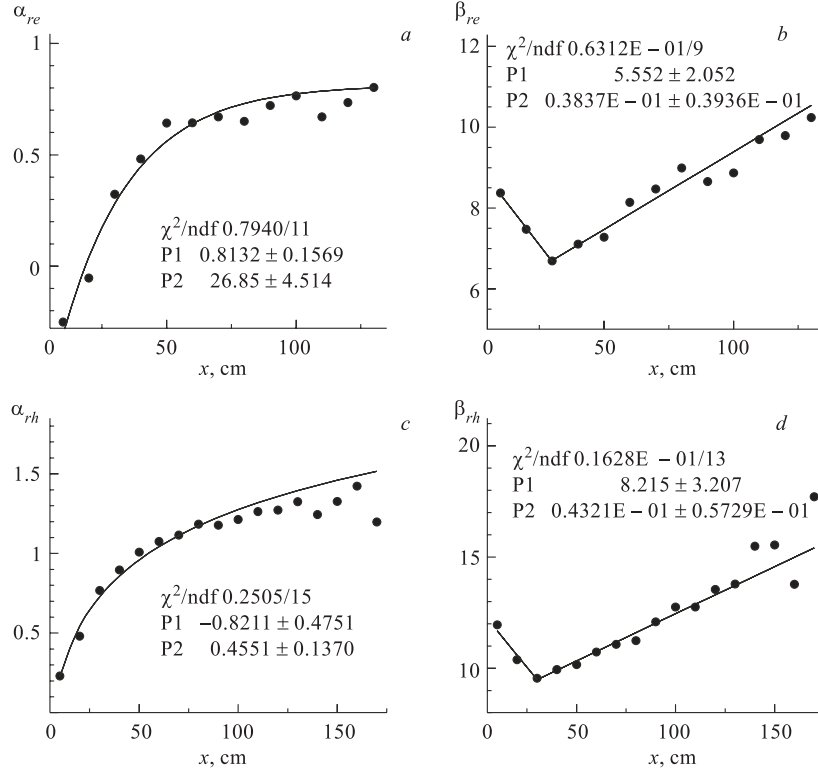


Fig. 10. Cases for electromagnetic and hadronic components: a) $\alpha_{re}(x)$; b) $\beta_{re}(x)$; c) $\alpha_{rh}(x)$; d) $\beta_{rh}(x)$

3.5. Shower Profile Parameters. Our method uses 25 parameters for description of shower profiles and their fluctuations:

- Two parameters for fluctuations of the π^0 energy fraction — α_w, β_w .
- Three parameters describing the average longitudinal electromagnetic component — $\alpha_e, \beta_e, \lambda_{\pi^0}$; and four parameters describing its fluctuations — $\sigma_{f1}, \mu_{f1}, c_e, d_e$.
- Two parameters describing the average longitudinal hadronic component — α_h, β_h ; and two parameters describing its fluctuations — c_e, d_e .
- Six parameters describing the radial electromagnetic profile — $\alpha_{e0}, \alpha_{e1}, \beta_{e1}, \beta_{e2}, \beta_{e3}, \beta_{e4}$.
- Six parameters describing the radial hadronic profile — $\alpha_{h0}, \alpha_{h1}, \beta_{h1}, \beta_{h2}, \beta_{h3}, \beta_{h4}$.

Using the GEANT program package, we have found their values for different incident energies (20, 50, 100, 200, 500 GeV). The study of the parameters of energy dependencies revealed that those dependencies are logarithmic, linear or constant:

$$\begin{aligned}
 P_i(E) &= p_i + q_i \ln E & \text{or} \\
 P_i(E) &= p_i + q_i E & \text{or} \\
 P_i(E) &= \text{const},
 \end{aligned}$$

where E is the incident energy in gigaelectronvolts; p_i and q_i have dimension of P_i . See Tables 3 and 4.

Table 3. The energy dependence of the longitudinal profile parameters

Parameter	Energy dependence
α_w	5.0
β_w	$0.102 - 0.0095 \ln E$
$\lambda_{\pi 0}$	$14.9 + 5.08 \ln E$
α_e	$1.83 + 0.333 \ln E$
β_e	$4.53 + 0.120 \ln E$
α_h	$0.81 + 0.147 \ln E$
β_h	$26.5 + 2.48 \ln E$
c_h	0.72
d_h	0.99
σ_{f1}	$0.72 - 0.068 \ln E$
μ_{f1}	$0.69 - 0.064 \ln E$
c_e	$0.455 - 0.181 \ln E$
d_e	0.20

Table 4. The energy dependence of the radial profile parameters

Parameter	Energy dependence
α_{e0}	$0.741 - 0.0811 \ln E$
α_{e1}	$-10.9 + 8.51 \ln E$
β_{e1}	$4.50 + 1.06 \ln E$
β_{e2}	$0.00130 - 0.0207 \ln E$
β_{e3}	$5.43 + 0.00177E$
β_{e4}	0.0274
α_{h0}	$-0.806 - 0.000581E$
α_{h1}	$0.571 - 0.0186 \ln E$
β_{h1}	$1.88 + 2.58 \ln E$
β_{h2}	$0.138 - 0.0601 \ln E$
β_{h3}	$2.80 + 1.16 \ln E$
β_{h4}	0.0527

4. COMPARISON WITH THE EXPERIMENTAL DATA

We tested the fast MC program based on the method described by simulation of the ATLAS hadronic Tile Calorimeter prototype response [5] on 50-, 100-, 200-, and 300-GeV π^- at $\theta = 10^\circ$.

We compared the fast simulation data with the experimental one from the test beam in 1995 [5].

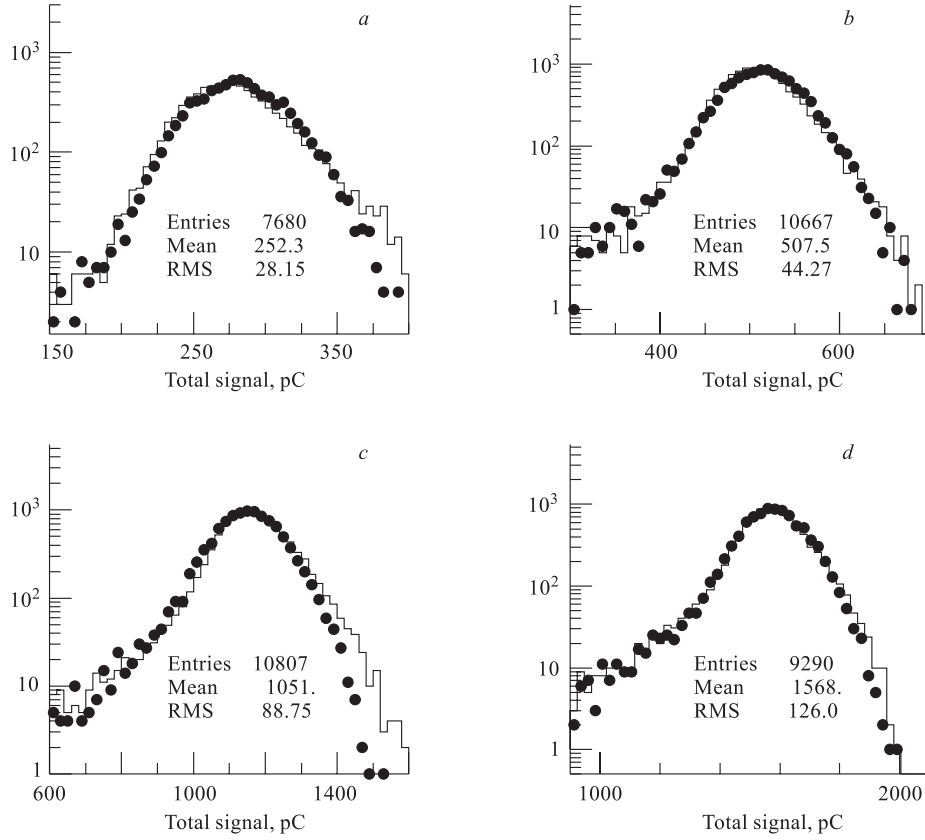


Fig. 11. The total signal for π^- , $E = 50$ (a), 100 (b), 200 (c), 300 GeV (d), respectively, $\theta = 10^\circ$. The histogram corresponds to the data, the black dots correspond to the fast MC simulation

In Fig. 11 the total signal in calorimeter calculated by the fast MC and those obtained at the experiment is compared. One can see that both the shape and the position of the peaks are in a good agreement. The left tail caused by energy leakage is well reproduced. The right tail, for which the noncompensation is responsible, is reproduced less successfully, especially in case of 50 GeV. The reason for this may be the limited validity of the formula (10).

In Fig. 12, the signals calculated by the fast MC and those obtained at the experiment in the individual calorimeter samplings for 100-GeV shower are compared. The signals from the different samplings represent the depth distribution of shower energy and thus enable us to test the shower longitudinal profile. A good agreement confirm correctness of our longitudinal profile analysis and the procedure of implementation of the longitudinal profile fluctuations. For the other energies (50, 200 and 300 GeV) agreement is very good, too.

The signal deposited in modules represents the radial distribution of energy. Modules 1 and 5 are the outermost ones. Only a small fraction of energy deposits in these two. In

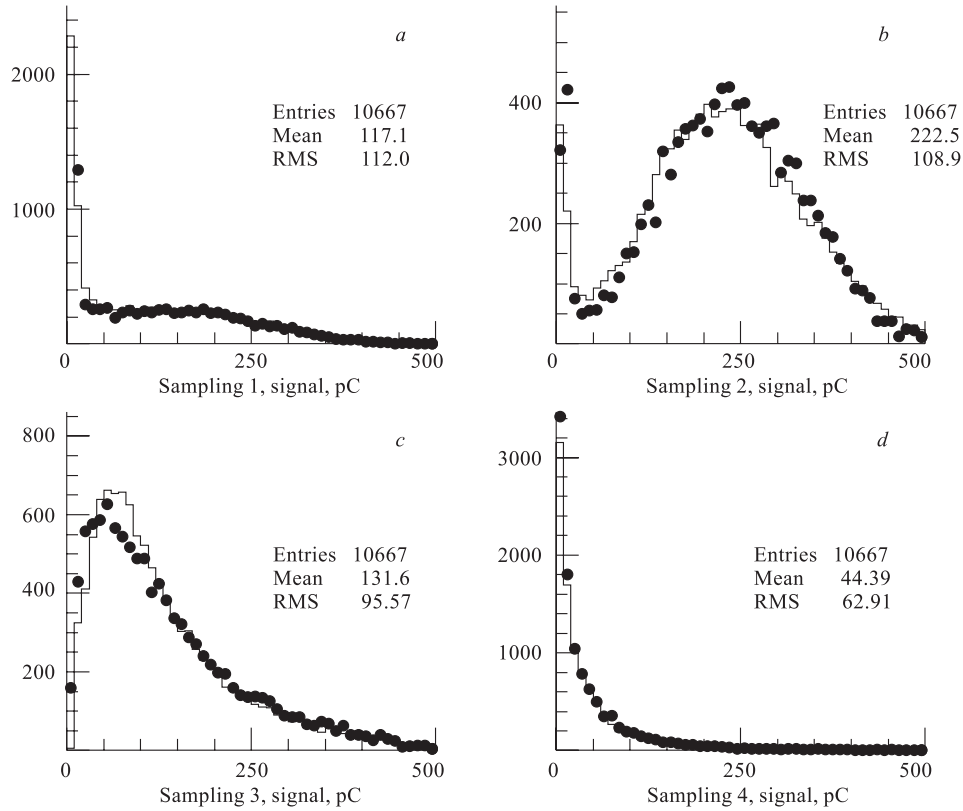


Fig. 12. The signal per sampling for π^- , $E = 100$ GeV, $\theta = 10^\circ$. The histogram corresponds to the data, the black dots correspond to the fast MC simulation

our fast MC method, only a few energy spots (e.g., 0 to 4 spots in 100-GeV shower) fall here, so the spectrum reproduces the data less successfully, especially in case of low incident energies. This is a limit of the method. In case of modules 2, 3 and 4 the fast MC spectra are narrower than the experimental ones (Fig. 13). The reason for this is that we did not include fluctuations of radial profiles as in case of longitudinal ones. The mean values of energy distributions agree sufficiently.

The signals from the calorimeter towers are compared in Fig. 14 for $E = 100$ GeV. The signal spectrum in tower 1 is not quite correct for the same reason as in modules 1 and 5. The signal spectra in other towers agree well for all energies (50, 100, 200 and 300 GeV), except for tower 2, where the distribution is narrower in fast MC.

The purpose of fast MC is to simulate hadronic shower development much faster than it is done by full simulations, e.g., GEANT. In Table 5 the simulation times for hadronic shower in calorimeter for carried out by the GEANT 3.21 and our fast MC are compared different energies. Our fast MC testing program is $3 \div 6 \cdot 10^3$ times faster than GEANT.

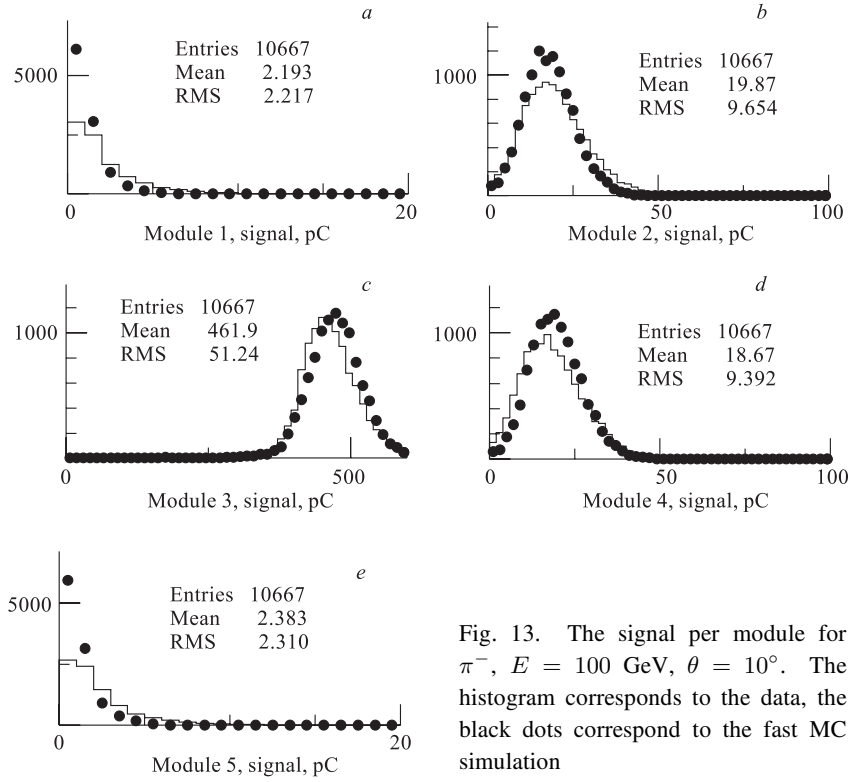


Fig. 13. The signal per module for π^- , $E = 100$ GeV, $\theta = 10^\circ$. The histogram corresponds to the data, the black dots correspond to the fast MC simulation

Table 5. The hadronic shower simulation times for the GEANT 3.21 code and the fast MC are compared; the calculations were carried out on the 1.5 GHz Intel Pentium 4

E , GeV	GEANT, s	Fast MC, s
50	15	$5 \cdot 10^{-3}$
100	40	$6 \cdot 10^{-3}$
200	65	$10 \cdot 10^{-3}$
300	80	$14 \cdot 10^{-3}$

CONCLUSION

The presented method of fast MC provides reliable and fast tool for simulating hadronic showers in sampling calorimeters. Although it has limits for low energies, it is able to correctly reconstruct the experimental data. The comparison of distributions of energy deposited in different depths along the shower axis proves correctness of the method of longitudinal shower fluctuations.

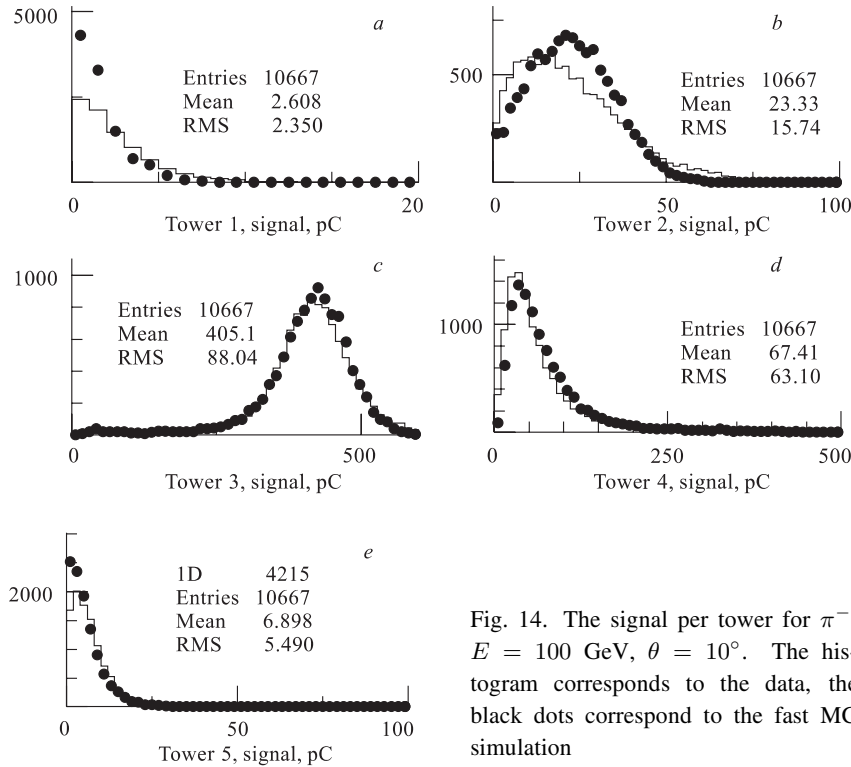


Fig. 14. The signal per tower for π^- , $E = 100$ GeV, $\theta = 10^\circ$. The histogram corresponds to the data, the black dots correspond to the fast MC simulation

Acknowledgements. The authors would like to thank J. Budagov and V. Vinogradov for valuable discussions and important comments. We are grateful to the ATLAS experiment community for interest in this work and important discussions.

REFERENCES

1. Brun R., Carminati F. GEANT Detector Description and Simulation Tool, W5013. CERN Program Library, Geneva.
2. Akhmadaliev S. et al. Hadronic Shower Development in Iron-Scintillator Tile Calorimetry // Nucl. Instr. Meth. A. 2000. V. 443. P. 51;
Budagov J. et al. Study of the Hadron Shower Profiles with the ATLAS Tile Hadron Calorimeter. ATL-TILECAL-1997-127. CERN. Geneva, 1997; JINR Preprint E1-97-318. Dubna, 1997.
3. Kulchitsky Y.A., Vinogradov V.B. Analytical Representation of the Longitudinal Hadronic Shower Development // Nucl. Instr. Meth. A. 1998. V. 413. P. 484.
4. Kulchitsky Y.A., Vinogradov V.B. On the Parameterization of Longitudinal Hadronic Shower Profiles in Combined Calorimetry // Nucl. Instr. Meth. A. 2000. V. 455. P. 499.
5. ATLAS Collab. ATLAS Tile Calorimeter Technical Design Report. CERN/LHCC/96-42. Geneva, 1996.

6. *Akhmadaliev S. et al.* Results from an Expanded Combined Test of the Electromagnetic Liquid Argon Calorimeter with a Hadronic Scintillating-Tile Calorimeter // Nucl. Instr. Meth. A. 2000. V. 449. P. 461;
Ajaltouni Z. et al. Results from a Combined Test of an Electromagnetic Liquid Argon Calorimeter with a Hadronic Scintillating Tile Calorimeter // Nucl. Instr. Meth. A. 1997. V. 387. P. 333;
Akhmadaliev S. et al. Hadron Energy Reconstruction for the ATLAS Calorimetry in the Framework of the Non-parametrical Method // Nucl. Instr. Meth. A. 2002. V. 480. P. 506.
7. *ATLAS Collab.* ATLAS Calorimeter Performance. CERN-LHCC-96-040. Geneva, 1996.
8. *ATLAS Collab.* ATLAS Detector and Physics Performance Technical Design Report CERN-LHCC-99-014. Geneva, 1999. V. 1.
9. *Grindhammer G., Rudowicz M., Peters S.* The Fast Simulation of Electromagnetic and Hadronic Showers // Nucl. Instr. Meth. A. 1990. V. 290. P. 469.
10. *Kulchitsky Y.A. et al.* The e/h Ratio of the ATLAS Barrel Tile Calorimeter. ATL-TILECAL-2001-001. Geneva, 2001; JINR Preprint E1-2002-13. Dubna, 2002.
11. *Budagov J. et al.* Electron Response and e/h Ratio of ATLAS Barrel Hadron Prototype Calorimeter. ATL-TILECAL-1996-072. Geneva, 1996; JINR Preprint E1-95-513. Dubna, 1995.
12. *Wigmans R.* Calorimetry-Energy Measurement in Particle Physics. N.Y.: Oxford University Press, 2000.
13. *Bock R.K., Hansl-Kozanecka T., Shah T.P.* Parametrization of the Longitudinal Development of Hadronic Showers in Sampling Calorimeters // Nucl. Instr. Meth. 1981. V. 186. P. 533.
14. *Wigmans R.* High Resolution Hadronic Calorimetry // Nucl. Instr. Meth. A. 1988. V. 265. P. 273.
15. *Juste A.* Analysis of the Hadronic Performance of the TILECAL Prototype Calorimeter and Comparison with Monte Carlo. ATL-TILECAL-1995-069. CERN. Geneva, 1995.

Received on May 20, 2003.